The EMBO Journal Vol.16 No.10 pp.2717–2729, 1997

Modulation of bacterial entry into epithelial cells by association between vinculin and the *Shigella* IpaA invasin

G.Tran Van Nhieu[1], A.Ben-Ze'ev[2] and P.J.Sansonetti

Unite de Pathogenie Microbienne Moleculaire, INSERM U389, Institut Pasteur, 28 rue du Dr Roux, 75724 Paris Cedex 15, France and [2]Department of Molecular Cell Biology, Weizmann Institute of Science, Rehovot 76100, Israel

[1]Corresponding author

Shigella flexneri **is the causative agent of bacillary dysentery in humans.** ***Shigella*** **invasion of epithelial cells is characterized by cytoskeletal rearrangements and formation of cellular projections engulfing the bacterium in a macropinocytic process. We show here that vinculin, a protein involved in linking actin filaments to the plasma membrane, is a direct target of** ***Shigella*** **during cell invasion. IpaA, a** ***Shigella*** **protein secreted upon cell contact, rapidly associates with vinculin during bacterial invasion. Although defective for cell entry, an** ***ipaA*** **mutant is still able to induce foci of actin polymerization, but differs from wild-type** ***Shigella*** **in its ability to recruit vinculin and α-actinin. Presumably, IpaA–vinculin interaction initiates the formation of focal adhesion-like structures required for efficient invasion.**

Keywords: actin polymerization/bacterial invasion/IpaA/*Shigella*/vinculin

Introduction

The ability to invade non-phagocytic cells is a critical virulence factor for enteroinvasive microorganisms. Several strategies have been devised by these pathogens to enter epithelial cells: some pathogens, such as *Yersinia pseudotuberculosis* and *Listeria monocytogenes*, enter cells by a zipper-like mechanism, in which the bacterium establishes intimate contact with the cell surface via an interaction between a single bacterial surface ligand and cellular receptors (Isberg, 1991; Isberg and Tran Van Nhieu, 1994; Mengaud *et al.*, 1996). This is in contrast to other enteropathogens, such as *Shigella* and *Salmonella*, for which entry into epithelial cells involves important cytoskeletal rearrangements at the area of bacterial interaction with the cell membrane. These rearrangements allow the formation of cellular extensions reaching several microns in length that rise around the bacterial body and allow its engulfment in a macropinocytic-like process (Finlay and Ruschkowski, 1991; Francis *et al.*, 1993; Adam *et al.*, 1995).

Shigella flexneri is an enteroinvasive bacterium responsible for a significant percentage of deaths related to diarrheal diseases worldwide. After ingestion, *Shigella* invades the colonic mucosa, where it induces an intense inflammatory reaction leading to destruction of the epithelium. The invasive properties of this bacterium have been linked to its ability to penetrate and spread from cell to cell (Clerc and Sansonetti, 1987; Bernardini *et al.*, 1989). As opposed to *Salmonella*, which remains confined and multiplies in intracellular vacuoles, *Shigella* lyses the phagocytic vacuole after internalization and multiplies in the cell cytosol. During this multiplication step, *Shigella* induces the formation of cellular protrusions pushing into adjacent cells, which allow infection of neighboring cells after lysis of the protrusion and the recipient cell membrane. In the case of *Shigella flexneri*, entry-associated genes are located on a 31 kb sequence of a 220 kb virulence plasmid (Maurelli *et al.*, 1985; Sasakawa *et al.*, 1988). Gene products encoded by the *mxi–spa* locus allow the formation of a specialized secretory apparatus specific for a subset of bacterial proteins (Parsot *et al.*, 1995) which are stored in the bacterial body and are secreted upon contact with the host cell (Menard *et al.*, 1994). Among these, Ipa proteins are critical for *Shigella* entry, as *ipaB*, *ipaC* and *ipaD* mutant *Shigella* strains are unable to enter epithelial cells (Sasakawa *et al.*, 1988; Menard *et al.*, 1993). Furthermore, inert particles coated with IpaB and IpaC complexes are readily internalized by cultured epithelial cells (Menard *et al.*, 1996), suggesting that these bacterial proteins are directly responsible for certain aspects of the bacterial entry process.

Interestingly, the pp60^{c-src} substrate actin binding protein cortactin is the major protein specifically tyrosyl phosphorylated during *Shigella* entry, which suggests activation of the pp60^{c-src} tyrosine kinase during the entry process (Dehio *et al.*, 1995). As several focal adhesion components are recruited at the site of *Salmonella* and *Shigella* entry (Finlay and Ruschkowski, 1991; Dehio *et al.*, 1995), some of which are substrates for pp60c-src (Clark and Brugge, 1995; Parsons, 1996), it is speculated that focal adhesion-like structures participate in *Shigella* entry. Consistent with this, the small G protein RhoA involved in focal adhesion and stress fiber formation (Nobes and Hall, 1995) has been shown to be involved in *Shigella*-induced cytoskeletal rearrangement during bacterial entry (Adam *et al.*, 1996). One proposed mechanism for focal adhesion induction by *Shigella* is association of the IpaB–IpaC–IpaD complex with the $\alpha_5\beta_1$ integrin (Watarai *et al.*, 1996). This association, however, does not appear to mediate significant binding of the bacterium to the cell surface (Watarai *et al.*, 1996) and is thus unlikely to allow bacterial internalization mediated by β_1 integrins based on high affinity receptor–ligand interactions. It is possible, however, that a combination of several signal transduction pathways is used by these pathogens during internalization by host cells. In fact, bacterial effectors may not use classical activation schemes via cell surface receptors and could potentially bypass inhibitor-sensitive steps. For example, homologs of the *mxi–spa* type III

secretory apparatus responsible for secretion of the Ipa proteins are also present in several other bacterial pathogens (Groisman and Ochman, 1993). In the case of *Yersinia*, the Ysc secretory apparatus is responsible for translocation of the Yops proteins from the bacterium to the cell cytosol upon cell contact (Rosqvist *et al.*, 1994). As *Shigella* proteins can be secreted *in vitro* via the *Yersinia* Ysc secretory apparatus (Rosqvist *et al.*, 1995), *Shigella* effectors responsible for entry may act by reaching an intracellular target after translocation into the cell cytosol.

We have investigated the role of the actin binding protein vinculin in *Shigella*-induced entry. Vinculin, a major component of adhesion structures, has been proposed as participating in anchorage of the cytoskeleton to the cell membrane by linking proteins such as α-actinin or talin via its head domain and F-actin with its tail domain (Menkel *et al.*, 1994; Johnson and Craig, 1995). Interestingly, vinculin also redistributes to focal complexes formed in response to growth hormone activation (Nobes and Hall, 1995), a process sharing similarities with *Salmonella* and *Shigella* invasion. We show in this report that *Shigella* entry into epithelial cells is a multi-step process involving different bacterial effectors and cellular responses. We have identified IpaA, a protein encoded by the *Shigella* invasion locus, as a bacterial effector of entry which rapidly associates with vinculin after bacteria–cell contact. Vinculin–IpaA interaction appears to be critical for efficient *Shigella* uptake, presumably by allowing recruitment of focal adhesion components to the site of bacterium interaction with the cell membrane. This IpaA-dependent recruitment could provide a molecular basis for the formation of focal complexes allowing anchorage of the bacterium within the entry structure.

Results

Vinculin expression is required for efficient entry of Shigella into host cells

To determine the role of vinculin in *Shigella*-induced entry, we first analyzed the ability of *Shigella* to induce internalization into the vinculin-deficient adenocarcinoma cell line ASML (Rodriguez Fernandez *et al.*, 1992) and ASML transfectants expressing chicken vinculin. Stable clones expressing significant levels of vinculin were isolated from three independent transfections with the plasmid pJ4Ω:vinc. Western blot analysis of the parental vinculin-deficient ASML cells confirmed that no detectable levels of vinculin were found in these cells, whereas their transfection with plasmid pJ4Ω:vinc encoding full-length chicken vinculin resulted in significant vinculin expression (not shown). The vinculin levels in these transfected clones were quantified by an ELISA-based assay (Materials and methods), using ASML mock-transfected cell as the baseline level (Figure 1A). As shown in Figure 1A, 14 cellular clones expressing significant levels of vinculin (Figure 1A, 1–14), showing up to a 4-fold variation among the different transfectants (Figure 1A, vinculin expression, compare clones 1 and 14), were isolated. Mock-transfected ASML cells and vinculin-transfected cells showed no obvious morphological differences and grew as rounded adherent cells when plated on plastic surfaces (not shown).

Monolayers of the same clones were tested for their ability to internalize *Shigella*. Adherent cells were challenged with *Shigella* strains and after incubation for 30 min at 37°C, the percentage of internalized bacteria was determined by the gentamicin protection assay (Isberg and Falkow, 1985). As shown in Figure 1B, cells expressing vinculin were able to internalize *Shigella* up to 10 times more efficiently than the vinculin-deficient ASML cells (compare solid bars and empty bar in Figure 1A and B respectively). This increase in internalization efficiency was dependent on the presence of the *Shigella* virulence plasmid, as a plasmid-cured *Shigella* strain did not show significant levels of internalization for both mock- and vinculin-transfected cells (not shown). The percentages of internalized bacteria in these different transfectants ranged from 0.25 to 1.2% (Figure 1B, clones 3 and 14) and were consistently higher than the values obtained for ASML cells transfected with the vector alone (Figure 1B, empty bar, ASML). When the values obtained in Figure 1B were plotted as a function of those of Figure 1A, a direct correlation was observed between the levels of vinculin expression and the levels of internalized bacteria (Figure 1C). Vinculin transfectants (Figure 1C, solid squares) that expressed low levels of vinculin still showed significant levels of internalization when compared with parental ASML cells (Figure 1C, empty square), but were less efficient at internalizing *Shigella* than clones expressing higher levels of vinculin. These results indicated that vinculin expression was required for efficient internalization of *Shigella* by host cells.

Purified vinculin binds the Shigella protein IpaA in a gel overlay assay

Previous work had shown that vinculin underwent a major redistribution in cells infected with *Shigella* and often co-localized with intracellular bacteria (Kadurugamuwa *et al.*, 1991). This suggested that bacterial effectors could interact with vinculin in the cell cytosol. To test this, we investigated the binding of vinculin to *Shigella* proteins separated by SDS–PAGE and transferred to an Immobilon-P filter.

Vinculin was purified from chicken gizzards as previously described (Evans *et al.*, 1984) with a few modifications. After purification, vinculin was radioiodinated and used to probe filters containing electrophoretically separated proteins from total bacterial extracts. As shown in Figure 2B, vinculin specifically bound to a 70 kDa *Shigella* protein present in extracts from wild-type *Shigella* (Figure 2B, lane 1) or extracts from the secretion defective *mxiD* mutant (Figure 2B, lane 3). This protein did not correspond to any major bacterial protein visualized by Coomassie staining (Figure 2A, lanes 1–4) and was encoded by the *Shigella* virulence plasmid, as no binding was observed with the plasmid-cured *Shigella* strain (Figure 2B, lane 2) or with *Escherichia coli* K12 (Figure 2B, lane 4). Also, the 70 kDa protein was abundantly secreted in the supernatant of a bacterial culture of an *ipaB Shigella* strain, a mutant that constitutively secreted proteins via the *mxi–spa* locus (Parsot *et al.*, 1995; Figure 2A and B, lane 5), but was absent from bacterial culture supernatant of a *Shigella* strain carrying a deletion of the *ipa* operon (Figure 2A and B, lane 6). These results indicated that the 70 kDa vinculin binding protein was encoded by the *Shigella* invasion locus *ipa*, which, from the estimated molecular weight, presumably corresponded to IpaA, a

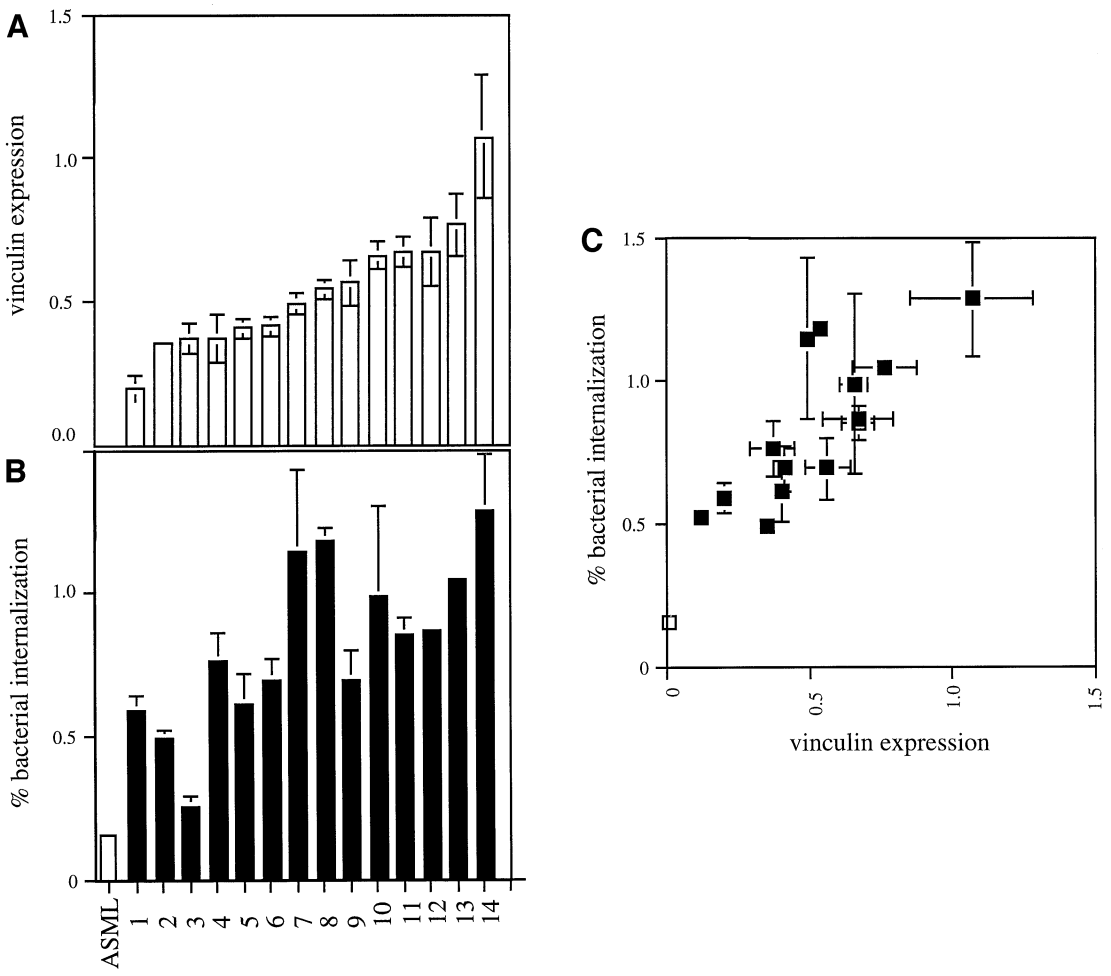

Fig. 1. Correlation between vinculin expression and *Shigella* entry into host cells. (**A**) Vinculin expression in stable ASML transfectants. Each transfectant was cloned and tested individually for vinculin expression using an ELISA-based assay using the anti-vinculin mAb vin11.5 and anti-mouse IgG coupled to peroxidase. For each transfectant, the cell density was quantitated by the crystal violet staining procedure (Brasaemle and Attie, 1988). Each value is the mean of three independent determinations. Vinculin expression values obtained from the anti-vinculin mAb ELISA-based assay normalized to cell density. (**B**) Percentage of *Shigella* internalization in the different transfectants. Cell monolayers were challenged with *Shigella* wild-type strain (M90T) for 30 min at 37°C. The percentage of internalized bacteria was quantitated using the gentamicin protection assay (Isberg and Falkow, 1985). No viable counts were detected when cells were infected with the non-invasive *Shigella* strain BS176. Each value is the mean of three independent determinations. ASML, parental cells; bars 1–14, individual vinculin transfectants; % bacterial internalization, percentage bacterial internalization determined by the gentamicin protection assay and normalized to cell density (Tran Van Nhieu and Isberg, 1993). (**C**) Correlation between bacterial internalization and the levels of vinculin expression. The values obtained in (B) were plotted as a function of the values obtained in (A). Empty square, ASML parental cells; solid squares, individual vinculin transfectants. There is a positive correlation between the levels of vinculin expression and the capacity of the cellular clones to internalize *Shigella.*

Shigella invasion locus encoded protein whose secretion had been shown to be triggered by host cell contact (Menard *et al.*, 1994). This was further confirmed by analysis of a *Shigella* mutant strain in which the *ipaA* gene was inactivated by plasmid insertion, which did not present vinculin binding activity (Figure 2B, lane 2).

An ipaA mutant strain of Shigella is deficient for entry, albeit entering cells at low levels independent of vinculin expression

Previous studies have indicated that inactivation of the *Shigella ipaA* locus resulted in strains that were still able to produce keratoconjunctivitis in hamsters (Sasakawa *et al.*, 1988). *ipaA* mutants, however, have a reduced plaque forming ability on cultured cell monolayers and are less virulent after injection into ligated rabbit intestinal loops (our unpublished results). One possible explanation for these apparent paradoxical results could be a defect in the invasion ability of the *ipaA* mutant which could not be detected in the keratoconjunctivitis test. As the IpaA protein directly bound vinculin in the gel overlay assay and because we had previously shown that vinculin was required for efficient internalization by host cells, we analyzed the entry phenotype of a *Shigella* strain in which the *ipaA* gene was mutated by insertional inactivation (Menard *et al.*, 1993).

As shown in Figure 3A, the *ipaA* mutant showed an ~10-fold decrease in its ability to invade HeLa cells (Figure 3A, *ipaA*) when compared with wild-type *Shigella* (Figure 3A, M90T). Internalization of the *ipaA* mutant, however, was not totally impaired (0.2%, Figure 3A, *ipaA*) and was significantly more efficient than that of the plasmid-cured strain (Figure 3A, BS176) or a mutant deficient for IpaB, another invasin encoded by the *ipa* locus that is critical for *Shigella* uptake (Figure 3A, *ipaB*). To confirm that the *ipaA* mutation caused a defect in the

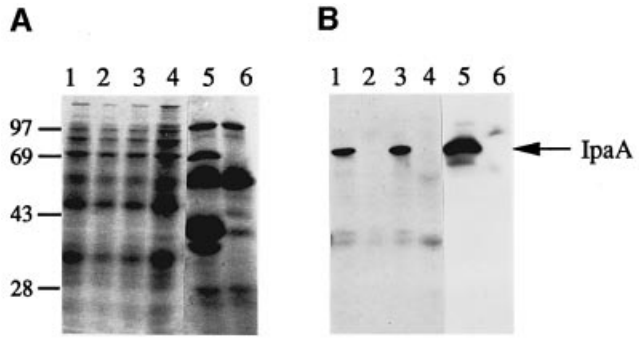

Fig. 2. Vinculin binding to the *Shigella* IpaA protein in a gel overlay assay. Gels containing whole bacterial extracts separated by SDS–PAGE were either stained with Coomassie blue (**A**) or duplicated on an Immobilon-P filter by electrotransfer and probed with [^{125}I]vinculin purified from chicken gizzards. Vinculin binding was detected by autoradiography (**B**). Lane 1, wild-type *Shigella* M90T; lane 2, *ipaA* mutant; lane 3, *mxiD* mutant, expressing the Ipa proteins but secretion defective; lane 4, *E.coli* MC1061; lane 5, supernatant from an *ipaB* mutant which constitutively secretes the other Ipa proteins as well as other Mxi–Spa secretion-dependent proteins (Parsot *et al.*, 1995); lane 6, supernatant of a Δ*ipa* mutant, constitutively secreting other Mxi–Spa secretion-dependent proteins, but with the *ipa* locus deleted. The binding of vinculin to the IpaA protein is indicated with an arrow (IpaA).

ability of the strain to induce entry and not decreased levels of association with host cells, the entry efficiency was analyzed on isogenic *Shigella* strains that were bound to the cell surface by means of the AfaE adhesin (Labigne-Roussel *et al.*, 1984). Bacterial internalization after short time periods of incubation with cells was quantitated by counting bacteria that were not accessible to anti-lipopolysaccharide (LPS) antibody in non-permeabilized cell samples. HeLa cells were incubated for 15 min at 21°C with wild-type *Shigella* or with an *ipaA* mutant expressing the afimbrial adhesin AfaE, to allow binding of the bacteria to the cell surface. Monolayers were shifted to 37°C to allow bacterial internalization and paraformaldehyde was added to the samples at different time points. After fixation, samples were incubated with anti-LPS antibodies with or without host cell permeabilization. As shown in Table I, ~30% of bound wild-type bacteria were internalized after 5 min at 37°C, versus only 3.6% for the *ipaA* mutant (Table I, Percent bacterial internalization). Longer incubations resulted in significant levels of bacterial internalization, with ~37% of the bacteria being internalized after 30 min for wild-type *Shigella* and 18% bacterial internalization for the *ipaA* mutant (Table I, Percent bacterial internalization).

These results indicate that although still capable of invading cells, the *ipaA* mutant strain was significantly impaired in its ability to induce entry into host cells. Expression of the AfaE adhesin, however, appeared to partially compensate for the entry defect linked to the *ipaA* mutation.

To analyze the *ipaA* invasive phenotype as a function of vinculin expression levels, vinculin-deficient ASML cells as well as three stable vinculin transfectants were analyzed for their ability to internalize wild-type *Shigella* strain or the *ipaA* mutant strain. As shown in Figure 3B, the entry efficiency of the *ipaA* mutant remained low in the different cells tested and was not significantly affected by expression of vinculin in the various transfectants

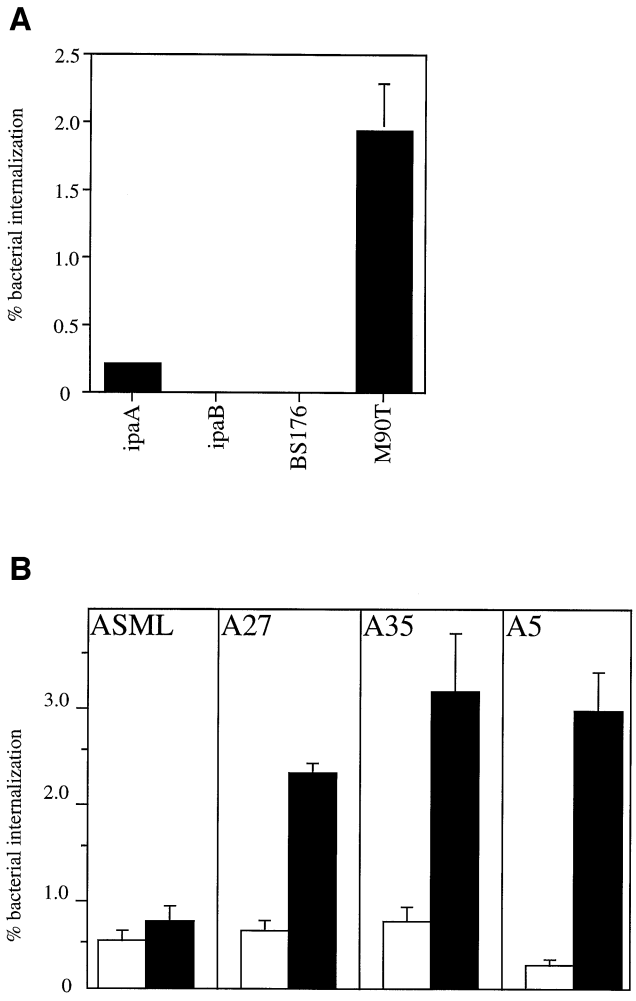

Fig. 3. The IpaA-deficient *Shigella* mutant enters cells with low efficiency and independently of vinculin expression. (**A**) HeLa cell monolayers were challenged with *Shigella* strains for 30 min at 37°C and the percentage of bacterial internalization was determined by the gentamicin protection assay. Each value is the mean of three independent determinations. Cells challenged with: ipaA, *ipaA* mutant; ipaB, *ipaB* mutant; BS176, plasmid-cured M90T; M90T, wild-type *Shigella*. The *ipaA* mutant is 10-fold less efficient in its ability to invade HeLa cells. (**B**) ASML cells and vinculin transfectants were challenged with wild-type *Shigella* or the *ipaA* mutant and the percentage bacterial internalization was determined by the gentamicin protection assay. Empty bars, cells challenged with the *ipaA* mutant; solid bars, cells challenged with wild-type *Shigella*; ASML, ASML parental cells transfected with the neomycin-resistant vector alone; A27, A35 and A5, individual vinculin transfectants. Each value is the mean of three independent determinations. In contrast to wild-type *Shigella*, the *ipaA* mutant does not show increased bacterial internalization in vinculin transfectants.

(Figure 3B, empty bars). These entry levels appeared to be comparable with the low levels of entry observed for the wild-type *Shigella* strain in the vinculin-deficient ASML parental cells (Figure 3B, ASML, compare the empty and solid bars). For the wild-type strain, however, cellular expression of vinculin allowed up to a 12-fold increase in bacterial internalization efficiency (Figure 3B, solid bars). These results indicate that at least two distinct steps occur during *Shigella*-induced entry: (i) one resulting in low levels of entry that is independent of the bacterial IpaA protein and vinculin expression; (ii) another dependent on vinculin and IpaA and required for efficient bacterial internalization.

Table I. Analysis of actin polymerization foci induced by wild-type *Shigella* and the *ipaA* mutant

	5 min	15 min	30 min
Percent bacterial internalization[a]			
Wild-type	26.1 ± 9.2	35.8 ± 9.1	36.9 ± 8.4
ipaA mutant	3.6 ± 1.0	12.2 ± 6.3	17.8 ± 2.5
Percent bacteria associated with actin polymerization foci[b]			
Wild-type	26.0 ± 0.1	1.3 ± 0.03	0
ipaA mutant	24.1 ± 0.08	24.3 ± 0.05	8.7 ± 0.08
Percent bacteria associated with actin coat structures[c]			
Wild-type	n.d.	23.8 ±8.6	46.3 ± 29.2
ipaA mutant	n.d.	1.2 ± 0.3	n.s.

Each value was obtained by counting ~500 bacteria in at least 10 fields from two independent experiments. n.d., not determined; n.s., not significant.
[a]The percentage of bacteria internalized was determined by labeling bacteria before and after detergent permeabilization with anti-LPS antibodies. Internalized bacteria were counted as bacteria that were unambiguously protected from labeling before permeabilization and expressed as the ratio of protected bacteria to the total number of cell-associated bacteria labeled after permeabilization.
[b]Ratio of bacteria associated with foci of actin polymerization to total number of cell-associated bacteria after double immunolabeling of the samples for F-actin and bacterial LPS.
[c]Ratio of bacteria partially or totally associated with an actin coat to total number of cell-associated bacteria.

IpaA associates with vinculin during Shigella infection

To analyze IpaA association with vinculin during *Shigella* invasion of epithelial cells, IpaA was purified from the supernatant of an *ipaD* mutant *Shigella* strain after SDS–PAGE and electroelution of the 70 kDa protein band. This material was used to immunize rabbits to produce anti-IpaA antiserum, which was used for immunoprecipitation of IpaA from extracts of cells infected with *Shigella*. The immunoprecipitates were then analyzed by Western blotting using anti-vinculin monoclonal antibody. As shown in Figure 4A, vinculin was specifically co-immunoprecipitated with the anti-IpaA antiserum in extracts of cells infected with the wild-type *Shigella* strain (Figure 4A, lane 4). The smaller vinculin cross-reacting species most probably represent degradation products. In contrast, only trace amounts of vinculin were immunoprecipitated with the anti-IpaA antibody in extracts from cells infected with the *ipaA* mutant strain (Figure 4A, lane 5) or from uninfected cells (Figure 4A, lane 6), indicating that co-immunoprecipitation of vinculin was specific for the IpaA protein. In reverse immunoprecipitation experiments in which vinculin was first immunoprecipitated from infected cells and the immunoprecipitates analyzed by Western blotting using anti-IpaA antiserum, IpaA co-immunoprecipitated with vinculin (Figure 4B, lane 4), although a few cellular species that cross-reacted with the anti-IpaA antiserum were also visible (Figure 4B). The other *Shigella* invasin, IpaB, was not detected in anti-vinculin antibody immunoprecipitates after Western blot analysis using an anti-IpaB antibody, (Figure 4C, lanes 4 and 5), while significant amounts of the IpaB protein were present in soluble extracts of cells infected with wild-type (Figure 4C, lane 7) or the *ipaA* mutant *Shigella* strains (Figure 4C, lane 8). In control experiments, bacterial cytoplasmic

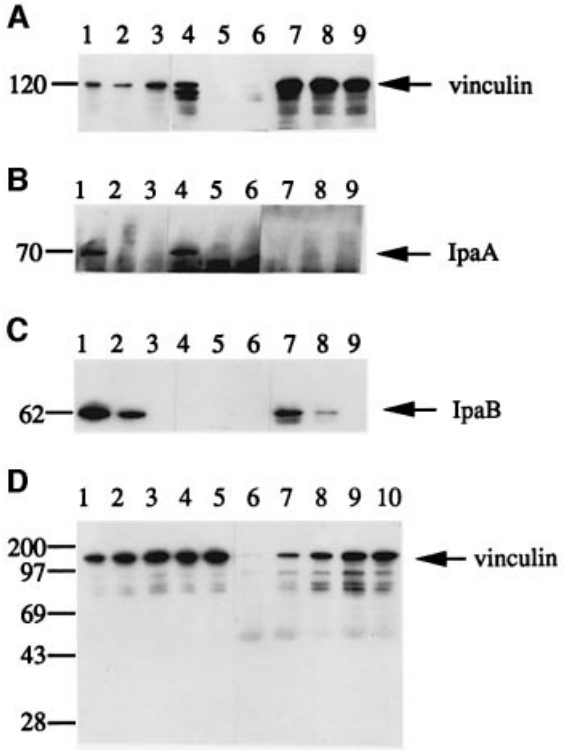

Fig. 4. IpaA associates with vinculin in HeLa cell extracts challenged with *Shigella*. To synchronize the infection, cell monolayers were infected with *Shigella* strains expressing the AfaE adhesin for 15 min at 21°C to allow binding. Samples were shifted to 37°C for 30 min to allow bacterial internalization. The cells were placed on ice, washed in ice-cold PBS and lysed in extraction buffer. After clearing by centrifugation, the pellet was saved (sample pellet) and cell lysates were subjected to immunoprecipitation. Immunoprecipitation supernatants (supernatants) were precipitated with 5% trichloroacetic acid. Immunoprecipitates were washed three times in extraction buffer, resuspended in Laemmli buffer and processed for Western blot analysis. Lanes 1–3, sample pellets; lanes 4–6, immunoprecipitates; lanes 7–8, supernatants. Lanes 1, 4 and 7, cells challenged with wild-type *Shigella*; lanes 2, 5 and 8, cells challenged with the *ipaA* mutant; lanes 3, 6 and 9, uninfected cells. (**A**) Immunoprecipitation using the anti-IpaA antibody and Western blot analysis using the anti-vinculin vin11.5 mAb. (**B**) Immunoprecipitation using anti-vinculin mAb and Western blot analysis using anti-IpaA antibody. (**C**) Immunoprecipitation using anti-vinculin mAb and Western blot analysis using anti-IpaB mAb. Bound antibodies were detected using the chemiluminescent ECL system. (**D**) HeLa cells were challenged with wild-type *Shigella* and cell lysates were prepared as above and subjected to immunoprecipitation using anti-IpaA antibody. Samples were processed for Western blot analysis using anti-vinculin mAb. Lanes 1–5, immunoprecipitation supernatants; lanes 6–10, immunoprecipitates. Lanes 1 and 6, cells challenged only at 21°C; lanes 2 and 7, cells shifted to 37°C for 5 min; lanes 3 and 8, 10 min; lanes 4 and 9, 15 min; lanes 5 and 10, 30 min. The arrow indicates the position of full-length vinculin. The molecular weights are indicated.

tryptophan synthase was exclusively found in the insoluble fraction of *Shigella*-infected cell extracts, with no detectable amounts in the soluble fraction (not shown), indicating that the presence of the Ipa proteins in the soluble cellular fraction was not due to bacterial lysis during the infection process.

To analyze the kinetics of IpaA association with vinculin during *Shigella* entry, experiments were performed in which HeLa cells were challenged with bacteria for various incubation periods at 37°C. Vinculin association with IpaA required incubation at 37°C, as samples that were kept at

21°C did not show significant levels of vinculin in anti-IpaA immunoprecipitates (Figure 4D, lane 6). When samples were shifted to 37°C, however, vinculin associated with IpaA within 5 min, with a steady increase in association over the first 15 min (Figure 4D, lanes 7–10). Prolonged incubation at 37°C resulted in significant degradation of vinculin associated with IpaA (results not shown). No significant changes in the soluble pool of vinculin were observed after precipitation with the anti-IpaA antibody during these experiments (Figure 4D, lanes 1–5), suggesting that only a small fraction of the total vinculin pool was involved in association with IpaA. No association of IpaA with α-actinin, another actin binding and focal adhesion protein, could be detected in similar co-immunoprecipitation experiments (data not shown). These results indicate that IpaA associates with vinculin early after cell contact and suggest that IpaA is translocated from the bacterium to the cell cytosol during entry.

Cytoskeletal reorganization linked to IpaA expression during Shigella internalization

To investigate the nature of the entry defect linked to IpaA deficiency, the ability of the *ipaA* mutant *Shigella* strain to induce actin polymerization at the site of bacterium–cell interaction was analyzed. Bacteria were incubated with HeLa cell monolayers, fixed at various time points and processed for double immunofluorescence staining of bacterial LPS and F-actin, followed by secondary incubation with phalloidin coupled to Bodipy (green) and anti-rabbit IgG coupled to Texas red (red). As shown in Figure 5a and d, bacteria-induced foci of actin polymerization were clearly visible after 5 min incubation at 37°C (Figure 5a and d, arrowheads). Unexpectedly, and although deficient for entry, the *ipaA* mutant was found to induce actin polymerization at a frequency similar to that of wild-type *Shigella* (Figure 5a and d, arrowheads), with ~24% of cell-bound bacteria being associated with a local reorganization of the cytoskeleton (Table I, Percent bacteria associated with actin polymerization foci, compare *ipaA* mutant and wild-type). With wild-type *Shigella*, however, the frequency of bacteria-induced actin polymerization foci decreased rapidly to 1.3% after 15 min incubation at 37°C (Figure 5b and Table I, Percent bacteria associated with actin polymerization foci, wild-type) and no detectable foci were observed after 30 min, as ~36% of the bacteria were internalized (Table I, Percent bacterial internalization, wild-type). In contrast, IpaA-deficient bacteria induced foci of actin polymerization to a similar extent after 15 min (Figure 5e) and foci were still detectable after 30 min incubation (Table I, Percent bacteria associated with actin polymerization foci, *ipaA* mutant).

Interestingly, the foci of actin polymerization induced by the *ipaA* mutant and wild-type *Shigella* showed strikingly different characteristics. In the case of wild-type *Shigella*, actin polymerization appeared to result in the formation of an organized structure surrounding the bound bacterium (Figure 5c). The cell membrane in intimate contact with the bacterium in the process of being internalized was coated with polymerized actin, as visualized by confocal microscopy analysis (Figure 5g, planes 1–3) and bacteria that were deeply engaged in the entry structure were also often coated with polymerized actin (Figure 5b, arrow). After internalization, a significant number of bacteria were found associated with such actin coat structures (Figure 5c and Table I, Percent bacteria associated with actin coat structures, wild-type). With the *ipaA* mutant, however, bacteria often associated with the periphery of actin polymerization foci (Figure 5f). In this latter case, these foci appeared to consist of microspike-like structures (Figure 5f) which did not organize as did foci induced by wild-type *Shigella* (Figure 5h, planes 1–5) and did not appear to be as productive for bacterial internalization (Table I, Percent bacterial internalization, *ipaA* mutant). As opposed to wild-type *Shigella*, actin coat structures were almost never found associated with *ipaA* mutant bacteria (Table I, Percent bacteria associated with actin coat structures).

IpaA-dependent recruitment of vinculin and α-actinin at Shigella-induced entry foci

As IpaA–vinculin interaction is critical for efficient *Shigella* entry, the recruitment of vinculin relative to IpaA localization was analyzed in entry foci induced by wild-type *Shigella* or the *ipaA* mutant.

Interestingly, vinculin was recruited to entry foci induced by wild-type *Shigella* (Figure 6A, vinculin, R), but also in foci induced by the *ipaA* mutant (Figure 6B, vinculin, R). With wild-type *Shigella*, however, vinculin often showed a strong staining close to bacteria being internalized (Figure 6A, red, 1–4) that was superimposable with staining of the actin coat (Figure 6A, green, 1–4). Although the average staining intensity of vinculin in the entry structure of the *ipaA* mutant appeared to be similar to that of wild-type *Shigella*, such an actin or vinculin coat was not found with the *ipaA* mutant (Figure 6B, vinculin, R and 1–4). These results suggest that although overall recruitment of vinculin to *Shigella*-induced entry foci did not appear to depend on IpaA, vinculin was specifically recruited to the close vicinity of the bacteria in an IpaA-dependent manner.

When stained with the anti-IpaA antibody, IpaA localized mostly in entry foci of cells infected with wild-type *Shigella* (Figure 6C, wt, IpaA), in a staining that co-localized with that of vinculin (Figure 6C, wt, vinculin) and F-actin (Figure 6C, wt, F-actin). Staining of the cell nuclear region was also observed with the anti-IpaA antibody, even after adsorption of the antiserum on HeLa cell extracts. This staining, however, was independent of IpaA and was probably due to cross-reacting cellular protein(s), as uninfected cells showed a similar staining with this antibody (not shown). Staining of bacteria-induced entry foci was specific for IpaA, as no staining was observed in foci induced by the *ipaA* mutant (Figure 6C, *ipaA*, IpaA).

When stained for α-actinin, a striking difference was observed between the wild-type and the *ipaA* mutant. With wild-type *Shigella*, α-actinin showed a strong recruitment in bacteria-induced entry foci (Figure 6D, α-actinin), which partially co-localized with actin staining (Figure 6D, F-actin + LPS, green). In contrast, α-actinin was recruited to the entry structure induced by the *ipaA* mutant to a much lesser extent (Figure 6E, α-actinin), although actin was polymerized to a significant extent (Figure 6E, F-actin + LPS). These results indicate that recruitment of α-actinin at *Shigella*-induced entry foci is dependent on IpaA and suggest that IpaA could promote efficient *Shi-*

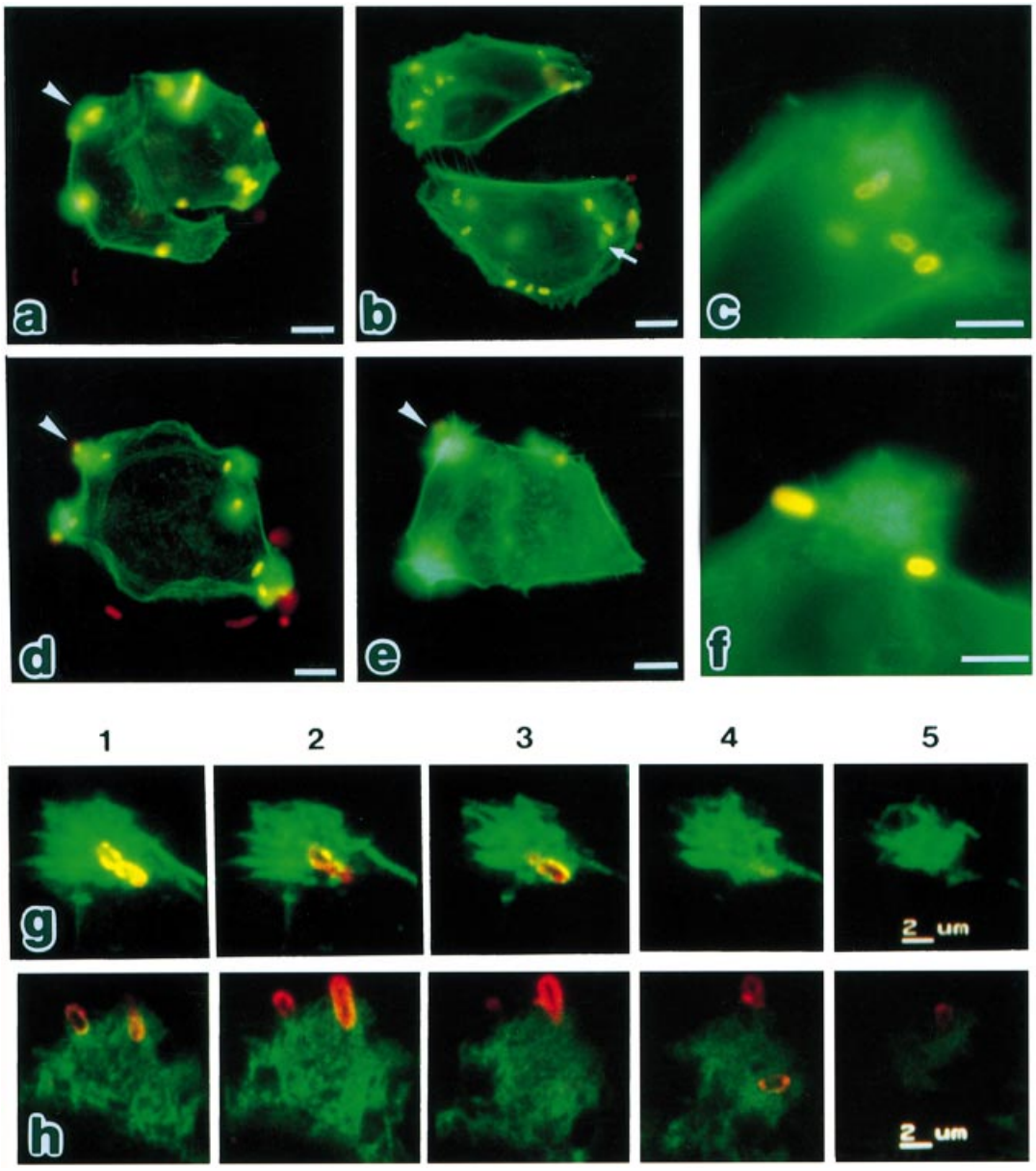

Fig. 5. Induction of actin polymerization foci by the *ipaA* mutant. HeLa cells were challenged with *Shigella* strains expressing the AfaE adhesin and shifted to 37°C for 5 min (**a** and **d**), 12 min (**c** and **f**–**h**) or 15 min (**b** and **e**). After incubation at 37°C, samples were fixed with 3.7% paraformaldehyde, permeabilized and processed for bacterial labeling using rabbit anti-LPS antibody and anti-rabbit IgG coupled to Texas red, as well as F-actin staining using Bodipy–phalloidin. (a–f) Direct fluorescence microscopy. (g and h) 1–5, optical sections interspaced by 1.5 μm obtained by confocal microscopy, parallel to the cell substratum starting from the basal (1) to the dorsal cell surface (5). (a–c and g) Cells challenged with wild-type *Shigella*. (d–f and h) Cells challenged with the *ipaA* mutant. Arrowheads indicate the formation of *Shigella*-induced structures corresponding to localized polymerization of actin. (a), (b), (d) and (e), bar = 10 μm; (c) and (f), 4 μm; (g) and (h), 2 μm. At early time points, the *ipaA* mutant induces the formation of polymerized actin foci at a frequency similar to that of the wild-type. Bacteria-induced foci of actin polymerization organized differentially for the *ipaA* mutant (f and h) when compared with wild-type *Shigella* (c and g), with bacteria often associated with the periphery of the foci (f and h). Actin structures coating the bacterium in the process of being internalized observed for wild-type *Shigella* (b, arrow, and g, 1–5, yellow staining) were not detected for the *ipaA* mutant (h, 1–5).

gella internalization by allowing recruitment of α-actinin, as well as vinculin and F-actin, close to the vicinity of the bacterium during internalization.

Discussion

A role for vinculin in Shigella entry

Vinculin is an important component of focal adhesion structures linking the cytoskeleton to the extracellular matrix, as well as microfilament-associated adherens junctions involved in cell–cell contact (Burridge *et al.*, 1988; Geiger and Ginsberg, 1991). The ability of vinculin to link F-actin appears to be regulated by intramolecular interaction between the vinculin tail, including the F-actin binding domain (Menkel *et al.*, 1994; Johnson and Craig, 1995), and the head domain. Anchoring of the cytoskeleton to the plasma membrane via the cytoplasmic domain of β_1 integrins depends on an activated 'opened form' of vinculin showing high affinity for talin via its head domain and for F-actin via its tail domain (Johnson and Craig,

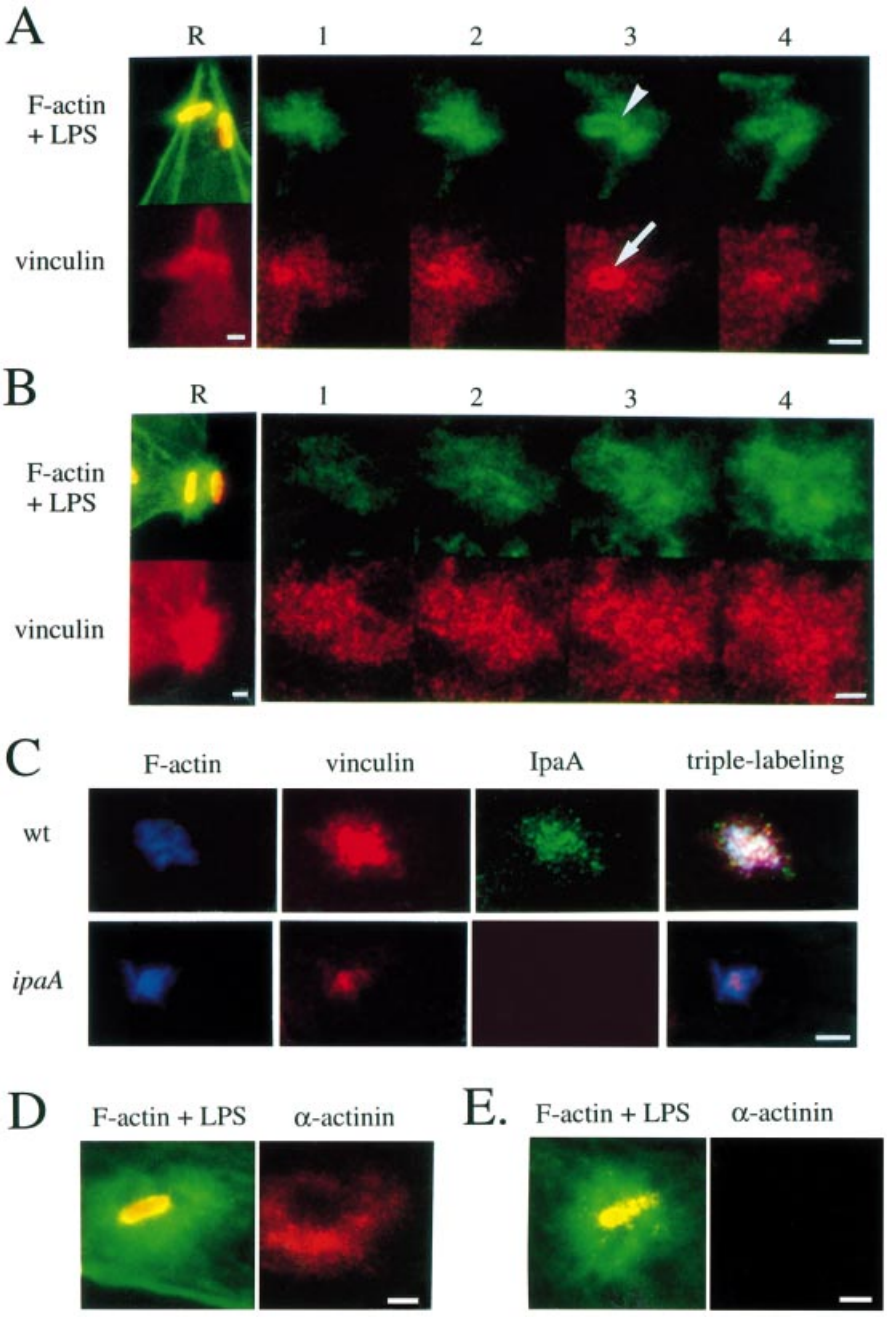

Fig. 6. Differential recruitment of vinculin and α-actinin in polymerized actin foci induced by the *ipaA* mutant and wild-type *Shigella*. HeLa cell monolayers were challenged with *Shigella* strains for 15 min at 21°C, followed by incubation for 12 min at 37°C. After incubation, the cells were fixed, permeabilized and processed for immunolabeling as described in Materials and methods. (**A**, **C** wt and **D**) Cells infected with wild-type *Shigella*. (**B**, **C** *ipaA* and **E**) Cells infected with the *ipaA* mutant. (A and B) F-actin+LPS, labeling of F-actin (green) and *Shigella* LPS (red); vinculin, vinculin labeling (red). (C) Labeling of F-actin (F-actin), vinculin (vinculin), IpaA (IpaA) or superimposition of the three labelings (triple labeling). (D and E) F-actin+LPS, labeling of F-actin (green) and *Shigella* LPS (red); actinin, α-actinin labeling. (A and B) 1–4, optical sections interspaced by 1.5 μm obtained by confocal microscopy, parallel to the cell substratum starting from the dorsal (1) to the basal cell surface (4); R, reconstructed image obtained by averaging the fluorescence from optical sections 1–4. (A), (B), (D) and (E), bar = 1 μm; (C), 2 μm. Foci of actin polymerization show reinforced vinculin (A, plane 3, arrow) and actin (A, plane 3, arrowhead) staining for both the wild-type and the *ipaA* mutant. The *ipaA* mutant-induced foci, however, do not show a strong reinforcement of vinculin staining in the close vicinity of the bacterium in the process of being internalized and only traces of α-actinin in the foci of actin polymerization.

1995). Although the molecular mechanisms are still unclear, the redistribution of vinculin from a cytoplasmic soluble pool to focal contacts in response to growth factor activation is linked to a change from an inactive to an activated state of vinculin, in a process involving tyrosine kinases, protein kinase C and the small G protein Rho (for a review see Craig and Johnson, 1996). In this study, we show that vinculin expression in cells is required for efficient *Shigella* internalization. IpaA directly binds purified vinculin and associates with vinculin during invasion of epithelial cells. Furthermore, IpaA-mediated enhancement of *Shigella* entry requires vinculin expres-

sion, as vinculin-deficient cells show similar levels of entry for wild-type *Shigella* and the *ipaA* mutant. These results strongly suggest that IpaA allows efficient internalization by binding to vinculin.

Previous analysis of IpaA inactivation indicated that *ipaA* mutant *Shigella* were able to spread from cell to cell and were able to induce keratoconjunctivitis in the hamster (Sasakawa *et al.*, 1988). In this report, we have identified IpaA as a *Shigella* invasin playing a major role in the entry process. Although still able to induce low levels of internalization, *ipaA* mutants are significantly impaired in their ability to enter epithelial cells and also appear to be less cytotoxic for epithelial cell monolayers after prolonged incubation (our unpublished results). In addition, preliminary experiments indicate that *ipaA* mutants are less virulent in the rabbit intestinal loop model (our unpublished results). These paradoxical results might reflect different sensitivity of the tests utilized. It is likely that the large inoculum of *Shigella* in the Sereny test could mask a requirement for optimal bacteria-induced internalization. From our studies it appears that IpaA mediates efficient internalization by binding vinculin and that vinculin is also critical for efficient uptake by the cell. As vinculin expression is also a limiting factor in the *Shigella* entry process, it is possible that *Shigella* internalization is very inefficient in a cell epithelium where a significant amount of vinculin is engaged in cellular junctions and adhesive structures.

Binding of IpaA to vinculin during cell invasion: translocation or intracellular secretion

Upon cell contact, *Shigella* Ipa proteins are rapidly secreted from the bacterium to the extracellular medium via a specific secretion apparatus (Menard *et al.*, 1994). This secretion apparatus appears to be functionally conserved in other enteropathogens, such as *Yersinia*, where it allows secretion of the anti-phagocytic Yop proteins (Rosqvist *et al.*, 1994), and *Salmonella*, which secretes effectors of entry homologous to the Ipa proteins (Hermant *et al.*, 1995; Kaniga *et al.*, 1995). Heterologous secretion of *Salmonella* proteins has also been shown to occur in *Yersinia* (Rosqvist *et al.*, 1995). In the case of *Yersinia*, the Yop proteins are translocated from the bacterium to the macrophage cytosol upon contact with the cell (Rosqvist *et al.*, 1994). It appears that, like the *Yersinia* Yop proteins, IpaA rapidly gains access to the cell cytosol upon cell contact, where it can modulate the entry process. Indeed, IpaA can be immunodetected in an entry structure induced by wild-type *Shigella* and interaction between IpaA and vinculin can be detected as early as 5 min after interaction between *Shigella* and host cells.

When the cells were treated with cytochalasin to prevent *Shigella* internalization, however, a significant reduction in the levels of vinculin and IpaA immunocomplexes was observed (data not shown). Therefore, a significant fraction of the IpaA pool that associates with vinculin may result from secretion by internalized bacteria. Consistent with intracellular secretion of IpaA, *ipaA* mutants do not induce an important redistribution of vinculin at the site of bacterial growth after prolonged growth in the cell cytosol (our unpublished results). It is possible that besides its effect on *Shigella* entry, the IpaA–vinculin interaction also plays a role in *Shigella* cell–cell spread. In that case, a combination of defects in entry and cell–cell spread would be responsible for the decreased virulence of *ipaA* mutants *in vivo*.

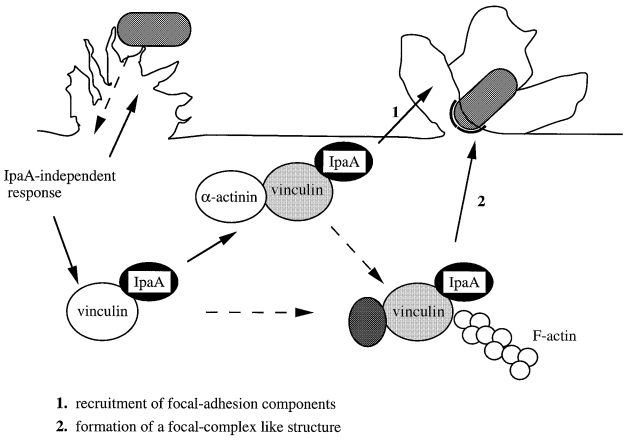

Fig. 7. IpaA-dependent reorganization of *Shigella*-induced entry foci. IpaA-independent factors induce actin polymerization and the recruitment of vinculin at foci that are non-productive for *Shigella* internalization (IpaA-independent response). IpaA association with vinculin allows recruitment of other cytoskeletal proteins such as α-actinin to cellular extensions organizing the entry structure (1), as well as the formation of a pseudo-focal adhesion at the membrane juxtaposing the bacterium (2).

A two-step Shigella-induced entry process

The fact that IpaA-deficient *Shigella* is still capable of inducing actin polymerization indicates that the initial events leading to cytoskeletal rearrangements are IpaA independent. As opposed to the *ipaA* mutant showing residual levels of internalization, *Shigella* strains mutated in the *ipaB*, *ipaC* and *ipaD* loci are totally impaired in their ability to enter epihelial cells (Sasakawa *et al.*, 1988; Menard *et al.*, 1993) and are unable to induce foci of actin polymerization. These results indicate that bacterial internalization mediated by IpaA depends on the activity of the other Ipa proteins and does not represent an alternate entry pathway. Thus, it is possible to distinguish between at least two events in *Shigella*-induced internalization: an initial event leading to actin polymerization which does not allow efficient *Shigella* uptake and an IpaA-dependent response that is required for efficient internalization (Figure 7). Interestingly, inert particles coated with the IpaB–IpaC complex can be internalized by HeLa cells, suggesting a direct effector role in the entry process for these *Shigella* invasins (Menard *et al.*, 1996). As particle uptake in this latter case appears to be rather inefficient in comparison with *Shigella* entry, it is possible that the IpaB and IpaC invasins are responsible for the non-productive actin polymerization foci leading to the residual levels of entry observed for the *ipaA* mutant. It is also possible that other *Shigella* factors modulate the entry process, as several bacterial proteins other than the Ipa proteins are translocated via the Mxi–Spa apparatus. For example, after prolonged incubation, the frequency of bacteria-induced foci of actin polymerization decreased rapidly with wild-type *Shigella*, while remaining more or less constant with the *ipaA* mutant. The implication of IpaA deficiency in this lasting induction is not clear: IpaA could play a direct role in down-modulation of these foci during *Shigella* entry or, alternatively, down-modulation

of actin polymerization foci induced by wild-type *Shigella* could be linked to secretion of other factors by internalized bacteria.

Modulation of Shigella-induced foci of actin polymerization by the IpaA–vinculin interaction

The analogy between membrane ruffling in response to growth factor stimulation and *Salmonella*-induced entry has led to the use of the term 'ruffling' to designate bacteria-induced membrane deformations at the site of entry, although in the latter case these membrane extensions form mostly on the dorsal surface of the cell. Interestingly, vinculin, along with talin, is recruited to focal complexes associated with filopodia and lamellipodia formed in response to growth factor activation (Ben-Ze'ev *et al.*, 1990; Nobes and Hall, 1995). In the case of neurite outgrowth, vinculin does not appear to play a role in the formation of these cellular extensions, but rather may be involved in their stabilization (Varnum-Finney and Reichardt, 1994). Because of the recruitment of vinculin to *Shigella*-induced foci of actin polymerization, it is possible that vinculin participates in stabilization of cellular extensions induced by *Shigella* during entry. Vinculin expression by itself, however, was not sufficient for productive *Shigella* uptake, as IpaA-deficient *Shigella* strains are inefficiently internalized by vinculin-expressing cells, with levels similar to those of wild-type *Shigella* in vinculin-deficient cells. In addition, vinculin appears to be recruited in foci of actin polymerization induced by the *ipaA* mutant to a similar extent as in foci induced by wild-type *Shigella*. It is conceivable that initial events induced by *Shigella* that lead to the formation of these IpaA-independent cellular projections also induce recruitment of vinculin to these structures. Therefore, the role of IpaA–vinculin interaction during *Shigella* entry appears to be more complex than a simple recruitment of vinculin to the *Shigella* entry site. In fact, the most striking difference between the wild-type and the *ipaA* mutant strains was the consistent vinculin coat surrounding the bacterial body for the wild-type strain, which was not found for the *ipaA* mutant strain. Instead of physically recruiting vinculin to the *Shigella* entry site, IpaA binding to vinculin could potentiate or modulate its activity, by favoring vinculin interaction with other actin binding proteins. These changes of vinculin activity may translate into two kinds of responses. On the one hand, via vinculin binding, IpaA could allow the recruitment of other components of focal adhesion complexes to the site of cytoskeletal rearrangements induced by *Shigella*. (Figure 7, 1). Consistent with this, the actin binding protein α-actinin is massively recruited to entry foci induced by wild-type *Shigella*, whereas it is recruited to foci induced by the *ipaA* mutant to a much lesser extent. On the other hand, the vinculin and actin coat structures found surrounding wild-type *Shigella* during entry suggest another response that allows docking of vinculin at the site of the nascent bacterial phagosome, which would require vinculin 'activation' by IpaA to occur (Figure 7, 2).

Vinculin–IpaA interaction as a switch towards a focal adhesion-like structure?

One of the most striking features of vinculin immunolocalization experiments was the presence of strong recruitment to the close vicinity of the bacterium, which was linked to IpaA expression. Interestingly, the presence of this vinculin coat also correlated with assembly of the F-actin coat and α-actinin-containing coat in an IpaA-dependent manner, since ~24% of the cell-associated bacteria were entirely or partially coated with actin in the case of wild-type *Shigella*, whereas the *ipaA* mutant almost never associated with such structures (Table I). It is difficult to establish the hierarchy of events leading to formation of the IpaA-dependent coat, as actin polymerization itself can influence the distribution of actin binding proteins. Direct binding of vinculin to IpaA, however, points to such an interaction as a candidate for an initial event leading to subsequent coating. For example, IpaA-specific recruitment of α-actinin at entry foci is likely to occur via vinculin, as α-actinin does not appear to associate with IpaA and has been shown to directly bind vinculin (Otto, 1983). Activation of vinculin by IpaA would permit anchorage of the cytoskeleton to the phagosomal membrane by a yet to be identified mechanism and initiate the organization of a focal adhesion-like structure, without which bacteria would be repelled by the formation of bacteria-induced cellular extensions most of the time. Interestingly, IcsA, the *Shigella* protein responsible for formation of an actin comet tail at one pole of the bacterium, has also been reported to bind vinculin (Suzuki *et al.*, 1996). As IpaA appears to be implicated in the recruitment of vinculin to the site of *Shigella* intracellular growth and to influence actin comet tail formation (our unpublished results), it is tempting to speculate that activation of vinculin by IpaA favors vinculin association with IcsA and allows the formation of a vinculin-rich structure required for elongation of actin filaments during intracellular motility.

Materials and methods

Bacterial strains, cell lines, plasmids, antibodies and reagents

Wild-type *Shigella flexneri* type 5 M90T and its derived strain BS176, cured of the virulence plasmid, were used in this study. The *ipaA* mutant was obtained by plasmid insertion in the *ipaA* gene (Menard *et al.*, 1993). *ipaB* and *ipaAD* mutants of *Shigella*, which constitutively secrete the Ipa proteins, were kindly provided by Claude Parsot. All bacterial strains were grown in trypticase soy broth at 37°C, unless otherwise stated. The pBR322-based p1018 plasmid encoding the AfaE adhesin and conferring resistance to spectinomycin was a kind gift from Chantal Lebouguenec (Insitut Pasteur, Paris, France). The eukaryotic expression vector pJΩ4:vinc carrying the chicken vinculin cDNA under the control of an LTR promoter has been described previously (Rodriguez Fernandez, *et al.*, 1992). The rat pancreas adenocarcinoma cell line ASML, showing no detectable levels of vinculin, was grown in RPMI medium (Gibco BRL) supplemented with non-essential amino acids and containing 10% fetal calf serum as described (Rodriguez Fernandez, *et al.*, 1992). HeLa cells were grown in minimal essential medium (Gibco BRL) containing 10% fetal calf serum. The anti-*Shigella* LPS monoclonal antibody (mAb) C20 was a kind gift from Armelle Phalipon. The anti-vinculin mAbs vin11.5 and hvin.1 were obtained from Sigma Chemical Co. The anti-α-actinin mAb BM-75.2 was from Biomakor. The anti-mouse IgG antibody and anti-rabbit IgG coupled to fluorescein or Texas red were from Amersham Corp. Protein G–Sepharose beads were from Pharmacia Ltd. The Bolton–Hunter reagent for radiolabeling was from Dupont NEN.

Transfection and analysis of vinculin expression levels in ASML cells

ASML cells were transfected as described previously (Rodriguez Fernandez *et al.*, 1992), using the lipofectin reagent (Pharmacia) and a ratio of 20:1 of the pJΩ4:vinc plasmid versus the pSV2neo plasmid to

allow selection. After 48 h, selective medium containing 0.5 mg/ml G418 (Pharmacia) was added to the transfection plates. Individual clones were isolated with a cloning ring after 8 days and expanded for vinculin expression analysis and for *Shigella* internalization assay. For each stable transfectant, vinculin expression was analyzed by trypsinizing a semi-confluent monolayer in a 100 mm tissue culture dish. The cells were washed twice in phosphate-buffered saline (PBS) and the equivalent of 10^6 cells was resuspended in 100 μl Laemmli loading sample buffer for Western blot analysis using the anti-vinculin mAb vin11.5, after SDS–PAGE on a 10% polyacrylamide gel. About 30% of the G418-resistant clones tested expressed detectable levels of full-length vinculin (not shown); clones which expressed high levels of vinculin also presented smaller anti-vinculin mAb cross-reacting species which could correspond to degradation products (not shown). Vinculin levels in the various transfectants were quantitated by an ELISA-based assay as described previously (Tran Van Nhieu and Isberg, 1993). Briefly, cells were seeded at a density of 5×10^5 cells/well in a 24-well tissue culture plate and were grown for 16 h to allow attachment to the plastic surface. Cell samples were then fixed in 3.7% paraformaldehyde for 20 min at 21°C, permeabilized with 0.1% Triton and processed for immunoprobing using the anti-vinculin mAb 11.5 at a concentration of 1.0 μg/ml in 25 mM HEPES, pH 7.3, in RPMI buffer containing 1% bovine serum albumin for 2 h at 21°C. After washing three times with PBS, the cells were incubated with peroxidase-coupled anti-mouse IgG antibody at a concentration of 10 μg/ml for 1 h at 21°C. Peroxidase activity was detected using the chromogenic OPD substrate and by reading absorbance at 405 nm using an ELISA reader (MR4000; Bio-Rad), after transferring the supernatant to a fresh 96-well plate. After peroxidase activity detection, the monolayers were rinsed twice with distilled water and the cell density in each well was determined by the crystal violet staining method (Brasaemle and Attie, 1988). Vinculin expression levels of each clone were normalized to cell density and expressed as the average ratio from at least three independent determinations of the values of peroxidase activity to the corresponding values obtained from crystal violet detection (Tran Van Nhieu and Isberg, 1993).

Bacterial entry analysis

Shigella internalization by cells was determined as described previously using the gentamicin protection assay (Isberg and Falkow, 1985). For short time periods (<30 min), however, internalization was quantitated visually by differentially counting cell-associated bacteria that were labeled with anti-LPS antibody before and after cell permeabilization. Bacteria expressing the AfaE adhesin (Labigne-Roussel, *et al.*, 1984) were allowed to bind to cells grown on coverslips for 15 min at 21°C at a multiplicity of infection of 10 bacteria/cell in 25 mM HEPES, pH 7.3, in minimal essential medium. After incubation, the medium was removed, fresh medium prewarmed to 37°C was added and the samples were shifted to 37°C. At given time points, samples were fixed with paraformaldehyde and first incubated with the anti-LPS mAb C20 for 60 min. Samples were then washed with PBS, permeabilized with 0.1% Triton X-100 for 7 min and further incubated with the anti-*Shigella* LPS antiserum for 60 min. Bound antobodies were then visualized after incubation with anti-mouse IgG coupled to fluorescein isothiocyanate (FITC) (Sigma Chemical Co.) and anti-rabbit IgG coupled to tetramethyl-rhodamine isothiocyanate (TRITC) (Amersham Corp.). Samples were mounted on slides using DABCO as a mounting reagent and analyzed using a fluorescence microscope (BH2-RFCA; Olympus Optical Co. Ltd) and filters specific for FITC (WIBA; Olympus), TRITC (WIY; Olympus) or a dual band filter (FITC & TRITC; Olympus).

Vinculin purification from chicken gizzards

Vinculin was purified from chicken gizzards as described previously (Evans *et al.*, 1984), with a few modifications. Briefly, gizzards were blended, washed in 0.5 mM phenylmethylsulfonyl fluoride (PMSF) and vinculin was extracted in 2 mM Tris, pH 9.0, containing 1 mM EDTA and 0.5 mM PMSF. The extract was clarified by precipitation using 10 mM $MgCl_2$ and the supernatant was concentrated by precipitation using ammonium sulfate at 20% final concentration before loading onto a DEAE–Sephacel (Bio-Rad) column. Vinculin was eluted using a low salt gradient (0–370 mM NaCl). The eluted fractions containing vinculin were pooled, dialyzed against 20 mM Tris, pH 7.5, containing 1 mM PMSF and 10 mM NaCl and loaded onto a HiLoad FPLC column. Vinculin was recovered in the flow-through. Vinculin was further concentrated using Centriprep 30 (Amicon) and stored at 4°C for short-term storage.

Preparation of bacterial extracts and vinculin overlay

Bacteria grown to early logarithmic phase (OD_{600} = 0.2) were harvested by centrifugation at 3000 *g* and resuspended in one tenth of the initial volume of Laemmli sample buffer (Laemmli, 1970) without reducing agents. Samples were boiled for 5 min before loading onto a standard 10% polyacrylamide gel and SDS–PAGE. After migration, proteins were transferred to an Immobilon-P filter using a semi-dry transfer system. Filters were blocked for 2 h in buffer containing 20 mM HEPES, pH 7.5, 10 mM NaCl, 15 mM β-mercaptoethanol, 1 mM EGTA, 0.05% sodium azide, 0.25% gelatin and 0.5% BSA. Vinculin binding to bacterial proteins was analyzed by a gel overlay technique (Otto, 1983), with a few modifications. Vinculin was radioiodinated using the Bolton–Hunter reagent for 15 min at 0°C in 0.125 M borate, pH 9.5, using 10 μCi/μg protein, and stored in PBS containing 0.1% BSA. After blocking, filters were incubated with purified ^{125}I-labeled vinculin at a final concentration of 1 μg/ml for 2 h at 21°C and subsequently washed three times in PBS containing 0.1% Tween 20 (PBS-T). Bound vinculin was revealed by autoradiography. Alternatively, vinculin binding was visualized by immunodetection. After incubation with non-radioactive vinculin, filters were incubated with the anti-vinculin mAb vin11.5 at 100 ng/ml in PBS-T for 60 min, washed three times in PBS-T and incubated with anti-mouse IgG antibody coupled to peroxidase. After washing with PBS-T, bound antibodies were detected using the ECL system (Amersham Corp.). The results were similar to those obtained with ^{125}I-labeled vinculin and vinculin binding to IpaA could be detected using this non-radioactive technique. This suggests that the binding observed was stable and specific for vinculin under the conditions used and that the vin 11.5 mAb does not interfere with vinculin–IpaA binding.

Production of the anti-IpaA antibody

IpaA was isolated from the culture supernatant of a *Shigella* strain for which the *ipaD* locus was inactivated and which constitutively secrete the Ipa proteins (Parsot *et al.*, 1995). Bacteria were grown in trypticase soy broth until late log phase (OD_{600} = 0.6) and the cells pelleted for 20 min at 4°C at 5000 *g*. The bacterial supernatant was filtered through a 0.22 μm nitrocellulose filter (Schleicher & Schull), the proteins were precipitated with ammonium sulfate at 60% final concentration, resuspended in one tenth of the original culture volume and dialyzed against three changes of 1 mM EDTA, 1 mM PMSF, 10 mM Tris, pH 7.5, at 4°C for 12 h. After adding Laemmli sample buffer and boiling for 5 min, the proteins were separated by SDS–PAGE on 10% polyacrylamide preparative gels, stained briefly using $CuCl_2$ (Lee *et al.*, 1987) and slices corresponding to the 70 kDa species were cut out and subjected to electroelution in Laemmli running buffer in dialysis bags. Electroeluted samples were concentrated using Centricon-30 (Amicon), dialyzed against PBS and the protein concentration was adjusted to 1 mg/ml. New Zealand rabbits were immunized using 100 μg protein/injection and antisera were tested after 2 months by Western blotting. To obtain anti-IpaA specific antibodies, antisera were adsorbed using nitrocellulose filters coated with bacterial extracts of *ipaA* mutant *Shigella*. Briefly, bacteria grown to late log phase were washed at 4°C in 10 mM Tris–HCl, pH 7.3, containing 1 mM PMSF and 1 mM EDTA and resuspended in one tenth of the original culture volume in the same buffer. All subsequent steps were carried out at 4°C. Bacteria were lysed by sonication in an ice bath, using three pulses of 20 s spaced by 30 s (output 6, Sonicator M234; MSE). Cell membranes and debris were pelletted at 100 000 *g* using a table-top ultracentrifuge (TL-100; Beckmann Corp.) and supernatants were directly incubated with nitrocellulose filters (5 ml/100 mm diameter filters) for 2 h. Filters were then blocked in PBS containing 1% BSA for 60 min. Two milliliters of antiserum were adsorbed by two successive 2 h incubations with these coated filters. Essentially the same procedure was used when adsorbing sera against cultured cell extracts, except that 10^7 cells were used to prepare extracts for each filter. The antibody obtained after immuno-adsorpation was specific for IpaA, as tested by Western blotting against whole bacterial extracts of wild-type *Shigella* and the IpaA-deficient strain (not shown). A 50 kDa cross-reacting species, however, was consistently seen when blotting against HeLa or 3T3 cell extracts, even after adsorption of the antibody against extracts prepared from these cell lines (not shown).

IpaA co-immunoprecipitation from Shigella-infected HeLa cell extracts

Bacteria were grown to OD_{600} = 0.8, washed once in PBS and resuspended at the same density in 25 mM HEPES, pH 7.3, minimal essential medium (MEM). HeLa cells grown to 60% confluency in 100 mm dishes were washed twice in PBS and resuspended in MEM–

HEPES for 90 min at 37°C. To synchronize the infection, cell monolayers were incubated with the bacterial suspensions for 15 min at 21°C and then shifted to 37°C. At different time points, the cell samples were chilled on ice, washed three times with ice-cold PBS containing 1 mM $MgCl_2$, 0.5 mM $CaCl_2$ and 1 mM Na_3VO_4 and scraped with a rubber policeman into 0.5 ml 0.1% Nonidet P-40, 1 mM PMSF, PBS (extraction buffer). Samples were homogenized using 10 strokes with a Dounce homogenizer (Size 1.8; Kontes Scientific Glassware, Vineland, NJ) and bacteria and cell membranes were pelleted by centrifugation for 5 min at 8000 *g* at 4°C. The supernatant was carefully transferred to a fresh tube and incubated with the anti-IpaA (1:100) or anti-vinculin vin11.5 mAb (5 µg/ml final concentration) for 90 min. Immune complexes were precipitated using 20 µl protein G–Sepharose beads (Pharmacia), washed three times in extraction buffer and resuspended in Laemmli sample buffer, before Western blot analysis.

Immunofluorescence confocal microscopy analysis

Samples were processed for triple immunofluorescence labeling. F-Actin was labeled using phalloidin conjugated to Bodipy. Vinculin and α-actinin were labeled with the h-vin.1 mAb (Sigma) or the BM-75.2 mAb respectively and anti-mouse IgG conjugated to TRITC. Bacteria were visualized using anti-LPS rabbit antiserum and anti-rabbit IgG conjugated to CY5. Fluorescent samples were analyzed using a confocal laser scanning microscope (Leica Inc., Deerfield, IL).

Acknowledgements

We thank Ralph Isberg for reviewing the manuscript. We are grateful to Claude Parsot and Robert Menard for providing mutant *Shigella* strains and for stimulating discussions and to Raymond Hellio for confocal microscopy analysis. We also thank Josette Arondel and Helene d'Hauteville for technical assistance in rabbit immunization and Armelle Phalipon for the gift of the anti-*Shigella* LPS mAb C20. This work was supported by a Pasteur–Weizmann collaboration grant and a grant from the Direction des Recherches et Techniques (94092).

References

Adam,T., Arpin,M., Prévost,M.C., Gounon,P. and Sansonetti,P.J. (1995) Cytoskeletal rearrangements and the functional role of T-plastin during entry of *Shigella flexneri* into HeLa cells. *J. Cell Biol.*, **129**, 367–381.

Adam,T., Giry,M., Boquet,P. and Sansonetti,P.J. (1996) Rho-dependent membrane folding causes *Shigella* entry into epithelial cells. *EMBO J.*, **15**, 3315–3321.

Ben-Ze'ev,A., Reiss,R., Bendori,B. and Gorodecki,B. (1990) Transient induction of vinculin gene expression in 3T3 fibroblasts stimulated by serum growth factors. *Cell Regulat.*, **1**, 621–636.

Bernardini,M.L., Mounier,J., d'Hauteville,H., Coquis-Rondon,M. and Sansonetti,P.J. (1989) Identification of *icsA*, a plasmid locus of *Shigella flexneri* that governs intra- and intercellular spread through interaction with F-actin. *Proc. Natl Acad. Sci. USA*, **86**, 3867–3871.

Brasaemle,D.L. and Attie,A.D. (1988) Microelisa reader quantitation of fixed, stained, solubilized cells in microtitre dishes. *BioTechniques*, **6**, 418–419.

Burridge,K., Fath,K., Kelly,G., Nuckolls,G. and Turner,C. (1988) Focal adhesions: transmembrane junctions between extracellular matrix and the cytoskeleton. *Annu. Rev. Cell Biol.*, **4**, 487–525.

Clark,E.A. and Brugge,J.S. (1995) Integrins and signal transduction pathways: the road taken. *Science*, **268**, 233–239.

Clerc,P. and Sansonetti,P.J. (1987) Entry of *Shigella flexneri* into HeLa cells: evidence for directed phagocytosis involving actin polymerization and myosin accumulation. *Infect. Immun.*, **57**, 2681–2688.

Craig,S.W. and Johnson,R.P. (1996) Assembly of focal adhesions: progress, paradigms, and portents. *Curr. Opin. Cell Biol.*, **8**, 74–85.

Dehio,C., Prevost,M.C. and Sansonetti,P.J. (1995) Invasion of epithelial cells by *Shigella flexneri* induces tyrosine phosphorylation of cortactin by a $pp60^{c\text{-}src}$ mediated signalling pathway. *EMBO J.*, **14**, 2471–2482.

Evans,R.R., Robson,R.M. and Stromer,M.H. (1984) Properties of smooth muscle vinculin. *J. Biol. Chem.*, **259**, 3916–3924.

Finlay,B.B. and Ruschkowski,S. (1991) Cytoskeletal rearrangements accompanying *Salmonella* entry into epithelial cells. *J. Cell Sci.*, **99**, 283–296.

Francis,C.L., Ryan,T.A., Jones,B.D., Smith,S.J. and Falkow,S. (1993) Ruffles induced by *Salmonella* and other stimuli direct macropinocytosis of bacteria. *Nature*, **364**, 639–642.

Geiger,B. and Ginsberg,D. (1991) The cytoplasmic domain of adherens-type junctions. *Cell Motil. Cytoskeleton*, **20**, 1–6.

Groisman,E.A. and Ochman,H. (1993) Cognate gene clusters govern invasion of host epithelial cells by *Salmonella typhimurium* and *Shigella flexneri*. *EMBO J.*, **12**, 3779–3787.

Hermant,D., Menard,R., Arricau,N., Parsot,C. and Popoff,M.Y. (1995) Functional conservation of the *Salmonella* and *Shigella* effectors of entry into epithelial cells. *Mol. Microbiol.*, **17**, 781–789.

Isberg,R.R. (1991) Discrimination between intracellular uptake and surface adhesion of bacterial pathogens. *Science*, **252**, 934–938.

Isberg,R.R. and Falkow,S. (1985) A single genetic lous encoded by *Yersinia pseudotuberculosis* permits invasion of cultured animal cells by *Escherichia coli* K-12. *Nature*, **317**, 262–264.

Isberg,R.R. and Tran Van Nhieu,G. (1994) Two mammalian cell internalization strategies used by pathogenic bacteria. *Annu. Rev. Genet.*, **27**, 395–422.

Johnson,R.P. and Craig,S.W. (1995) F-actin binding site masked by the intramolecular association of vinculin head and tail domains. *Nature*, **373**, 261–264.

Kaniga,K., Trollinger,D. and Galan,J.E. (1995) Identification of two targets of the type III protein secretion system encoded by the *inv* and *spa* loci of *Salmonella typhimurium* that have homology to the *Shigella* IpaD and IpaA proteins. *J. Bacteriol.*, **177**, 7078–7085.

Kadurugamuwa,J.L., Rohde,M., Wehland,J. and Timmis,K.N. (1991) Intercellular spread of *Shigella flexneri* through a monolayer medriated by membranous protrusions and associated with reorganization of the cytoskeletal protein vinculin. *Infect. Immun.*, **59**, 3463–3471.

Labigne-Roussel,A.F., Lark,L., Schoolnik,G. and Falkow,S. (1984) Cloning and expression of an afimbrial adhesin (AFA) responsible for P blood group-independent mannose-resistant hemagglutination from a pyelonephritic *E. coli* strain. *Infect. Immun.*, **46**, 251–259.

Laemmli,U.K. (1970) Cleavage of structural proteins during assembly of the head of bacteriophage T4. *Nature*, **227**, 680–685.

Lee,C., Levin,A. and Branton,D. (1987) Copper staining: a five-minute protein staining for sodium-dodecyl sulfate polyacrylamide gels. *Anal. Biochem.*, **166**, 308–312.

Maurelli,A.T., Baudry,B., d'Hauteville,H., Hale,T.L. and Sansonetti,P.J. (1985) Cloning of plasmid DNA sequences involved in invasion of HeLa cells by *Shigella flexneri*. *Infect. Immun.*, **49**, 164–171.

Menard,R., Sansonetti,P.J. and Parsot,C. (1993) Non polar mutagenesis of the *ipa* gene defines IpaB, IpaC and IpaD as effectors of *Shigella flexneri* entry into epithelial cells. *J. Bacteriol.*, **175**, 5899–5906.

Menard,R., Sansonetti,P.J. and Parsot,C. (1994) The secretion of the *Shigella flexneri* Ipa invasins is induced by the epithelial cell and controlled by IpaB and IpaD. *EMBO J.*, **13**, 5293–5302.

Menard,R., Prevost,M.-C., Gounon,P., Sansonetti,P. and Dehio,C. (1996) The secreted Ipa complex of *Shigella flexneri* promotes entry into mammalian cells. *Proc. Natl Acad. Sci. USA*, **93**, 1254–1258.

Mengaud,J., Ohayon,H., Gounon,P., Mege,R.-M. and Cossart,P. (1996) E-cadherin is the receptor for internalin, a surface protein required for entry of *L. monocytogenes* into epithelial cells. *Cell*, **84**, 923–933.

Menkel,A.R., Kroemker,M., Bubeck,P., Ronsiek,M., Nikolai,G. and Jockusch,B.M. (1994) Characterization of an F-actin-binding domain in the cytoskeletal protein vinculin. *J. Cell Biol.*, **126**, 1231–1240.

Nobes,C.D. and Hall,A. (1995) Rho, Rac, and Cdc42 GTPases regulate the assembly of multimolecular focal complexes associated with actin stress fibers, lamellipodia, and filopodia. *Cell*, **81**, 53–62.

Otto,J.J. (1983) Detection of vinculin-binding proteins with an ^{125}I-vinculin gel overlay technique. *J. Cell Biol.*, **97**, 1283–1287.

Parsons,T.J. (1996) Integrin-mediated signalling: regulation by protein tyrosine kinases and small GTP-binding proteins. *Curr. Opin. Cell Biol.*, **8**, 146–152.

Parsot,C., Menard,R., Gounon,P. and Sansonetti,P.J. (1995) Enhanced secretion through the *Shigella flexneri* Mxi-Spa translocon leads to assembly of extracellular proteins into macromolecular structures. *Mol. Microbiol.*, **16**, 291–300.

Rodriguez-Fernandez,J.L., Geiger,B., Salomon,D., Sabanay,I., Zoller,M. and Ben-Ze'ev,A. (1992) Suppression of tumorigenicity in transformed cells after transfection with vinculin cDNA. *J. Cell Biol.*, **119**, 427–438.

Rosqvist,R., Magnusson,K.E. and Wolf-Watz,H. (1994) Target cell contact triggers expression and polarized transfer of *Yersinia* YopE cytotoxin into mammalian cells. *EMBO J.*, **13**, 964–972.

Rosqvist,R., Hakansson,S., Forsberg,A. and Wolf-Watz,H. (1995) Functional conservation of the secretion and translocation machinery for virulence proteins of yersiniae, salmonellae and shigellae. *EMBO J.*, **14**, 4187–4195.

Sasakawa,C., Kamata,K., Sakai,T., Makino,S., Yamada,M., Okada,N. and Yoshikawa,M. (1988) Virulence-associated genetic regions comprising 31 kilobases of the 230-kilobase plasmid in *Shigella flexneri* 2a. *J. Bacteriol.*, **170**, 2480–2484.

Suzuki,T., Saga,S. and Sasakawa,C. (1996) Functional analysis of VirG domains esential for interaction with vinculin and actin-based motility. *J. Biol. Chem.*, **271**, 21878–21885.

Tran Van Nhieu,G. and Isberg,R.R. (1993) Bacterial internalization mediated by β1 chain integrins is determined by ligands affinity and receptor density. *EMBO J.*, **12**, 1887–1895.

Varnum-Finney,B. and Reichardt,L. (1994) Vinculin-deficient PC12 cell lines extend unstable lamellipodia and filopodia and have a reduced rate of neurite outgrowth. *J. Cell Biol.*, **127**, 1071–1084.

Watarai,M., Funato,S. and Sasakawa,C. (1996) Interaction of Ipa proteins of *Shigella flexneri* with α5β1 integrin promotes entry of the bacteria into mammalian cells. *J. Exp. Med.*, **183**, 991–999.

Received on October 2, 1996; revised on February 6, 1997